

The Magnetic Moment of K^{40} and the Hyperfine Structure Anomaly of the Potassium Isotopes*

J. T. EISINGER, B. BEDERSON, AND B. T. FELD

Research Laboratory of Electronics and Department of Physics, Massachusetts Institute of Technology, Cambridge, Massachusetts

(Received December 6, 1951)

The nuclear magnetic moment and atomic hyperfine splitting of the rare K^{40} isotope have been measured by the atomic beam magnetic resonance technique. Detection of K^{40} atoms, from a source of normal potassium, was achieved by employing a conventional surface ionization detector as the ion source for a mass spectrometer, and by utilizing an electron multiplier to count the K^{40} ions. By measuring the frequencies of appropriate lines in the Zeeman pattern, the nuclear moment was determined to be $\mu_I = -1.2964 \pm 0.0004$ nuclear magnetons. The hyperfine splitting in the ground state was redetermined, with higher precision than that of previous measurements, to be $\Delta\nu = 1285.790 \pm 0.007$ Mc/sec.

The ratio of the nuclear g factors of K^{39} and K^{40} was measured directly by observing, in the same homogeneous magnetic field, H , the frequencies of two lines (a doublet) in the Zeeman spectrum of each isotope. The doublet separation of these lines is, in each case, proportional to $2g_I\mu_0H$, so that the ratio of the doublet splittings yielded directly $|g(K^{40})/g(K^{39})| = 1.24346 \pm 0.00024$. From these results and from the previously measured $\Delta\nu(K^{39})$,

the hyperfine structure anomaly of these K isotopes is

$$\left\{ \frac{[2I(K^{40})+1]g(K^{40})\Delta\nu(K^{39})}{[2I(K^{39})+1]g(K^{39})\Delta\nu(K^{40})} \right\} - 1 = (0.466 \pm 0.019) \text{ percent.}$$

The theory of the hyperfine structure anomaly, as developed by A. Bohr and V. F. Weisskopf, has been applied to the interpretation of this result. The predictions of a number of specific models, previously suggested to account for the observed nuclear g factors, have been compared with this experiment and with previous results on the anomalies for the Rb and the abundant K isotopes. The "asymmetric core" model of A. Bohr gives the best over-all agreement, mainly on the basis of the K^{41} - K^{39} anomaly. In general, all models which are, in their essential features, based on the independent-particle model with spin-orbit coupling, give predictions in fair qualitative agreement with the experiments. The contribution of K^{40} to the hfs anomaly seems, however, to be (fortuitously) insensitive to the differences between the models investigated.

I. INTRODUCTION

THE interaction of the nuclear magnetic moment with the moment due to the orbital electrons causes the ground state of an atom with electronic angular momentum $J\hbar = \frac{1}{2}\hbar$ to be split into two hyperfine levels characterized by the total angular momentum quantum numbers $F = I \pm \frac{1}{2}$. Fermi and Segrè,¹ assuming the nuclear moment to be a point dipole, calculated the energy separation between these two levels to be

$$h\Delta\nu = \frac{8\pi}{3} \frac{(2I+1)}{I} \frac{m}{\mu_I\mu_0^2} \frac{m}{M} |\psi(0)|^2, \quad (1)$$

where μ_0 is the Bohr magneton, μ_I is the nuclear magnetic moment in nuclear magnetons (nm), $\psi(0)$ is the normalized electronic wave function at the nucleus, and m/M is the ratio of electron mass to proton mass. If the subscripts 1 and 2 denote two isotopes of the same element, then since $\psi(0)$ will be identical for the two isotopes,²

$$\frac{\Delta\nu_1}{\Delta\nu_2} = \frac{(2I_1+1)g_1}{(2I_2+1)g_2} \quad (2)$$

where $g = \mu_I/I$ is the nuclear g -factor.

Kopferman³ and Bitter⁵ have pointed out that if the finite size of the nucleus is taken into account, $\Delta\nu$ will

depend on the spatial distribution of the nuclear magnetic dipole, and the right side of Eq. (1) must be multiplied by a correction factor $1+\epsilon$, where ϵ depends on the magnetic dipole distribution over the nucleus. If this effect is taken into account, Eq. (2) must be replaced by

$$\frac{\Delta\nu_1}{\Delta\nu_2} = \frac{(2I_1+1)g_1}{(2I_2+1)g_2} (1+\Delta) \quad (3)$$

where $\Delta \cong \epsilon_1 - \epsilon_2$, is a measure of the hfs anomaly and depends on the nuclear structures of isotopes 1 and 2.

Bohr and Weisskopf⁴ have shown how the measurement of Δ leads to information about the structures of the nuclei involved. Their theory accounts for the hfs anomaly observed between Rb⁸⁵ and Rb⁸⁷ by Bitter⁵ and a similar anomaly for K^{39} and K^{41} reported by Ochs, Logan, and Kusch.⁶

The addition of one neutron to the K^{39} nucleus profoundly affects the static properties of the nucleus; the spin changes from $\frac{3}{2}$ to 4 and the magnetic moment changes from $+0.39$ nm to -1.24 nm. A comparison of the $\Delta\nu$ and g_I values for K^{39} and K^{40} might therefore be expected to reveal a considerable anomaly of the type discussed above. The $\Delta\nu$ of K^{40} , $\Delta\nu$ of K^{39} , and μ_I of K^{39} have previously been measured.⁷⁻⁹ A direct measurement of $\mu_I(K^{40})$ had, however, never been attempted, owing to the small natural abundance of

* This work has been supported in part by the Signal Corps, Air Materiel Command, and ONR.

¹ E. Fermi and E. G. Segrè, *Z. Physik* **82**, 729 (1933).

² Nuclear mass effects on the hfs are at least an order of magnitude smaller than any of the effects here considered.

³ H. Kopferman, *Kernmomente* (Akademische Verlagsgesellschaft, M.B.H., Leipzig, 1940), p. 17.

⁴ A. Bohr and V. F. Weisskopf, *Phys. Rev.* **77**, 94 (1950).

⁵ F. Bitter, *Phys. Rev.* **76**, 150 (1949).

⁶ Ochs, Logan, and Kusch, *Phys. Rev.* **78**, 184 (1950).

⁷ J. R. Zacharias, *Phys. Rev.* **61**, 270 (1942); Davis, Nagle, and Zacharias, *Phys. Rev.* **76**, 1068 (1949).

⁸ P. Kusch and H. Taub, *Phys. Rev.* **75**, 1477 (1949).

⁹ T. L. Collins, *Phys. Rev.* **80**, 103 (1950).

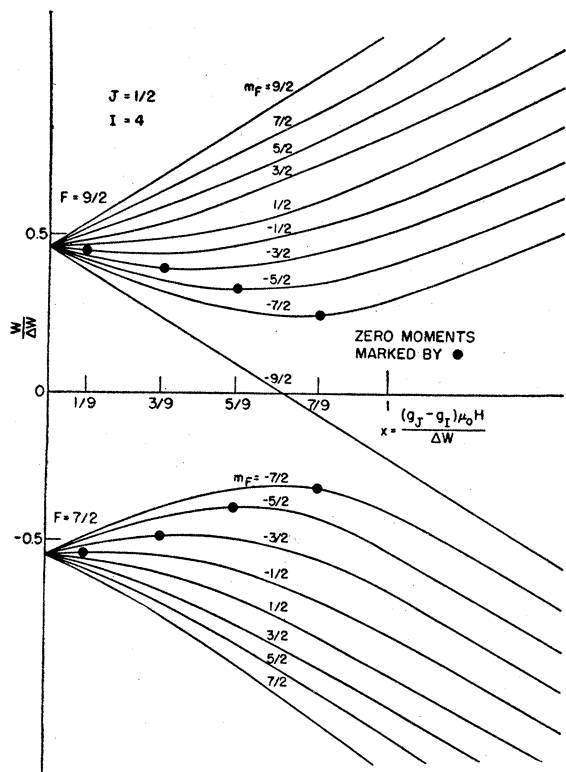


FIG. 1. Energy levels of the K^{40} atom as a function of an external magnetic field.

K^{40} (0.01 percent of ordinary K), which makes the isotope unsuitable for nuclear induction methods. It was therefore decided to measure the ratio $g(K^{40})/g(K^{39})$ by the atomic beam technique. The experiment also includes a direct measurement of $\mu_I(K^{40})$ and a remeasurement of $\Delta\nu(K^{40})$.

II. ENERGY LEVELS

The energy levels $W(F, m_F)$ of an atom with $J = \frac{1}{2}$ in an external magnetic field H are given by the Breit-Rabi formula¹⁰

$$\frac{1}{h}W(F = I \pm \frac{1}{2}, m_F) = -\frac{\Delta\nu}{2(2I+1)} + \frac{g_I \Delta\nu m_F x}{g_J - g_I} \pm \frac{\Delta\nu}{2} \left(1 + \frac{4m_F x}{2I+1} + x^2 \right)^{\frac{1}{2}}, \quad (4)$$

where $x = [(g_J - g_I)\mu_0 H]/h\Delta\nu$, g_J is the Landé g -factor for the electronic configuration, and g_I is the nuclear Landé g factor.¹¹ Figure 1 shows the energy levels of a K^{40} atom ($J = \frac{1}{2}$, $I = 4$) as a function of an external magnetic field.

The frequencies corresponding to transitions between

¹⁰ G. Breit and I. I. Rabi, Phys. Rev. **38**, 2072 (1931).

¹¹ The nuclear Landé g factor is defined as minus the ratio of the nuclear moment in Bohr magnetons to the nuclear spin, i.e., $g_I = -g(m/M)$.

states $m_F = -5/2$ and $m_F = -7/2$ are readily computed to be

$$\begin{aligned} \nu_+ &= \frac{1}{h} \left[W\left(\frac{9}{2}, -\frac{5}{2}\right) - W\left(\frac{9}{2}, -\frac{7}{2}\right) \right] \\ &= \frac{\Delta\nu}{2} \left[\left(1 - \frac{10}{9}x + x^2\right)^{\frac{1}{2}} - \left(1 - \frac{14}{9}x + x^2\right)^{\frac{1}{2}} \right] + \frac{g_I \Delta\nu x}{g_J - g_I} \quad (5) \end{aligned}$$

and

$$\begin{aligned} \nu_- &= \frac{1}{h} \left[W\left(\frac{7}{2}, -\frac{5}{2}\right) - W\left(\frac{7}{2}, -\frac{7}{2}\right) \right] \\ &= \frac{\Delta\nu}{2} \left[\left(1 - \frac{10}{9}x + x^2\right)^{\frac{1}{2}} - \left(1 - \frac{14}{9}x + x^2\right)^{\frac{1}{2}} \right] - \frac{g_I \Delta\nu x}{g_J - g_I}. \quad (6) \end{aligned}$$

Thus, the transitions belonging to $F = I \pm \frac{1}{2}$ are identical except for the last (nuclear) term, which appears with opposite signs in ν_+ and ν_- . The transitions given by Eqs. (5) and (6) therefore constitute a doublet whose separation is

$$\delta\nu = 2g_I \Delta\nu x / (g_J - g_I) = 2g_I \mu_0 H / h. \quad (7)$$

The K^{39} ($I = \frac{3}{2}$) atom in a magnetic field exhibits a pair of transitions similar to the above, given by

$$\begin{aligned} \nu_+ &= \frac{1}{h} [W(2, 0) - W(2, -1)] \\ &= \frac{\Delta\nu}{2} [(1+x^2)^{\frac{1}{2}} - (1-x+x^2)^{\frac{1}{2}}] + \frac{g_I \Delta\nu x}{g_J - g_I} \quad (5a) \end{aligned}$$

and

$$\begin{aligned} \nu_- &= \frac{1}{h} [W(1, 0) - W(1, -1)] \\ &= \frac{\Delta\nu}{2} [(1+x^2)^{\frac{1}{2}} - (1-x+x^2)^{\frac{1}{2}}] - \frac{g_I \Delta\nu x}{g_J - g_I}. \quad (6a) \end{aligned}$$

It is seen from Eq. (7) that if the field is kept constant during the course of a run consisting of measurements of ν_+ and ν_- of both K^{39} and K^{40} , the ratio of the g 's can be determined from

$$\delta\nu(K^{40})/\delta\nu(K^{39}) = g_I(K^{40})/g_I(K^{39}) = g(K^{40})/g(K^{39}). \quad (8)$$

Moreover, if the field at which the transitions characterized by Eqs. (5) and (6) occur is known, the doublet separation will yield the nuclear g -factor of K^{40} directly. The field dependence of these transitions is shown in Figs. 2 and 3.¹²

III. THE OBSERVATION OF TRANSITIONS

The atomic beam apparatus as used in this experiment is a high resolution radiofrequency spectrometer suitable for the observation of the transitions discussed

¹² Note that the constant of proportionality between x and the magnetic field H is different for K^{39} and K^{40} .

in the preceding section. A well-collimated beam of neutral atoms is made to pass through three magnetic fields, the A , C , and B fields, in that order, before being measured by the detection apparatus. The A and B fields have gradients in the same direction which are sufficiently large to produce measurable deflections of atoms whose effective magnetic moments are of the order of 0.1 Bohr magneton. The C field is a homogeneous field on which is superimposed an oscillating perturbing field capable of inducing transitions in the atoms of the beam. If an atom is made to undergo a transition of such a nature that in its new state it has an effective magnetic moment of opposite sign to that which it had in its original state, its deflection in the B field will be opposite to that which it suffered in the A field. Such atoms can be caused to strike the detector and are said to be refocused; the transitions are rendered observable by an increase of the beam intensity at the detector ("flop-in" transitions).

The K^{40} transitions which are of interest in the present experiment occur between the energy levels $(F, -5/2)$ and $(F, -7/2)$. As can be seen from Fig. 1, these energy levels have slopes and therefore effective magnetic moments of the same sign at all fields except between the "zero-moment" fields, for which $x=5/9$ and $x=7/9$.¹³ Flop-in transitions can therefore be

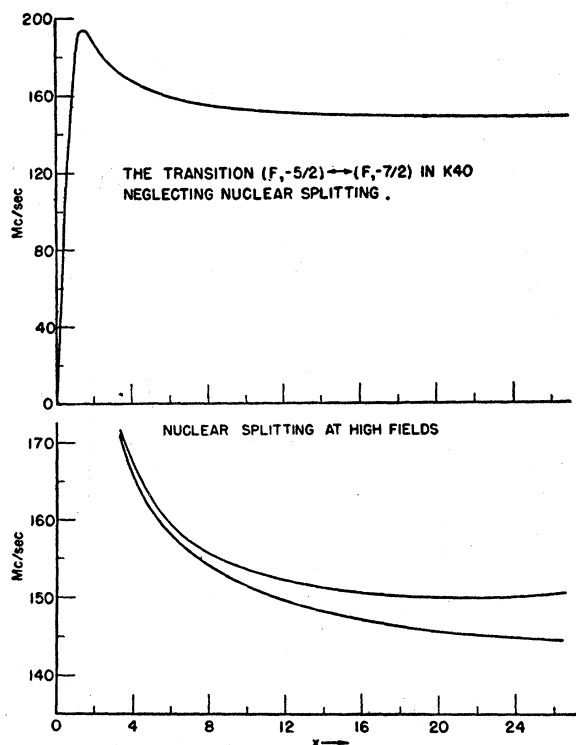


FIG. 2. The field dependence of the K^{40} doublet, the separation of which was measured in order to determine $g(K^{40})$. x is a parameter which is proportional to the external magnetic field.

¹³ It can be readily shown from the Breit-Rabi formula that the effective moment, $\mu_{\text{eff}} = -\partial W(F, m_F)/\partial H$ for an atom in the state (F, m_F) , vanishes in fields given by $x = -2m_F/(2I+1)$.

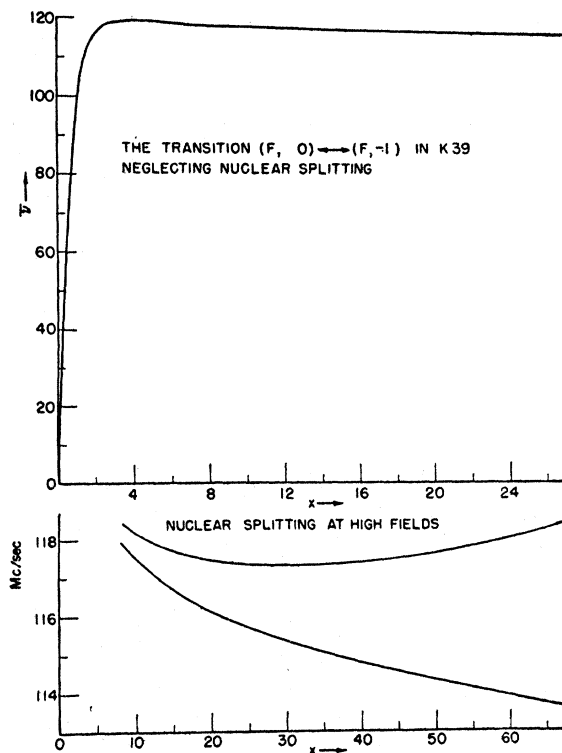


FIG. 3. The field dependence of the K^{39} doublet, the separation of which, when compared to the K^{40} doublet separation, gives $g(K^{40})/g(K^{39})$.

observed if $x \approx \frac{2}{3}$ for the A and B fields. Alternatively, the deflecting fields can be adjusted to have the value $x=7/9$. K^{40} atoms in the $m_F = -7/2$ state will then not be deflected by the A or B fields. If such an atom is made to undergo a transition to the state $m_F = -5/2$, it will have a finite effective moment in the B field and will be deflected away from the detector ("zero-moment flop-out" transitions).

IV. THE APPARATUS

The apparatus¹⁴ on which these experiments were performed has the following characteristics: The vacuum system consists of a brass casting ten feet long and one foot in diameter. The main chamber, which contains the magnets and detection apparatus, is usually at a pressure of 3×10^{-7} mm Hg and is separated from the poorer vacuum of the oven chamber by a partition chamber. The schematic drawing of Fig. 4 indicates the physical arrangement and the pumping system of the apparatus.

The oven for the production of the K beam is $2\frac{1}{2}$ inches high and $\frac{3}{4}$ inch in diameter. It is made of steel and is provided with a slit which is 6 mils wide. A few turns of tungsten wire heat the oven to about 450°C .

¹⁴ This apparatus, including the deflecting magnets and the mass spectrometer, was designed by Dr. Hin Lew while a member of this laboratory.

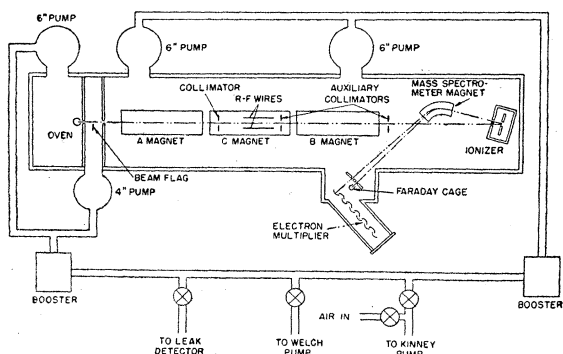


FIG. 4. Schematic diagram to illustrate the atomic beam apparatus used in the present experiment.

When loaded with two grams of K metal, it provided an intense steady beam for about 60 hours.

The *A* and *B* magnets, which are essentially the same length (25 and 26 inches, respectively), are single-turn electromagnets; a copper current sheet completely encloses the iron core except for two openings which allow the beam to pass between the pole faces. This construction assures a minimum amount of stray field in the transition region. The gradients are produced in the conventional manner¹⁵ by means of curved pole faces; their magnitudes are given by the expression $|\nabla H| = 1.57H$ gauss cm^{-1} .

The *C* magnet is 26 inches long, and its gap is $1\frac{1}{2}$ inches high by $\frac{1}{4}$ inch wide. The oscillating field is produced by passing a radiofrequency current through a pair of copper conductors; the beam passes between the conductors. The radiofrequency field so produced is about 15 cm in length. The windings of all magnets are water-cooled and energized by submarine storage batteries.

After passing through the magnets, the K atoms strike a hot tungsten filament and are converted into positive ions at its surface. The ions are accelerated from the filament, which is at a variable positive potential, through a slit held at ground potential and subsequently pass between the pole faces of a 60° mass spectrometer magnet which separates the various isotopes in the ion beam. The intensity of the ion beam corresponding to any particular isotope is then measured by means of a probe connected to the grid of an FP 54-electrometer tube. Very small beam intensities are measured by an electron multiplier¹⁶ connected to a multistage scaler. Figure 5 shows a mass spectrometer curve obtained in the present apparatus. The enrichment factor, defined as the intensity of the K^{39} beam divided by the residual amount of K^{39} beam at the K^{40} position, is about 5×10^4 . The normal K^{39} beam intensity was of the order of 10^{-10} amp, and the corresponding K^{40} beam gave a count of the order of 600 counts per second.

¹⁵ Rabi, Kellog, and Zacharias, *Phys. Rev.* **46**, 157 (1934).

¹⁶ H. Lew, *Phys. Rev.* **76**, 1086 (1949).

The transitions studied in this experiment are only moderately field dependent at high fields (Figs. 2 and 3). As a result, the resonance lines showed no broadening because of inhomogeneities in the *C* field, and it was possible to achieve resonance curves whose half-widths were equal to the theoretical half-widths as given by the uncertainty principle. For an oven temperature of 800°K , the beam atoms spend an average time of 3×10^{-4} second in the transition region, and the theoretical half-width of a resonance curve is 3 kc/sec. Figure 6 shows a typical resonance curve. The peaks of such curves could be determined to within 1 kc/sec by observing the change in counting rate as the frequency of the oscillating field was varied through the resonance.

The observed frequencies were in the neighborhoods of 115 Mc/sec, 150 Mc/sec, and 190 Mc/sec. Radiofrequency currents of the required stability were produced by mixing an accurately known fixed high frequency (120, 150, and 180 Mc/sec, respectively) with variable low frequencies. The fixed frequencies were obtained by multiplying the signal produced by a 5 Mc/sec crystal which was kept within one cycle per second of the 5 Mc/sec signal transmitted by WWV, so that the accuracy of the fixed frequency was about 2 parts in 10^7 .

The variable signal was produced by a General Radio 805C signal generator and was measured by a General Radio 620A wave meter. A General Radio

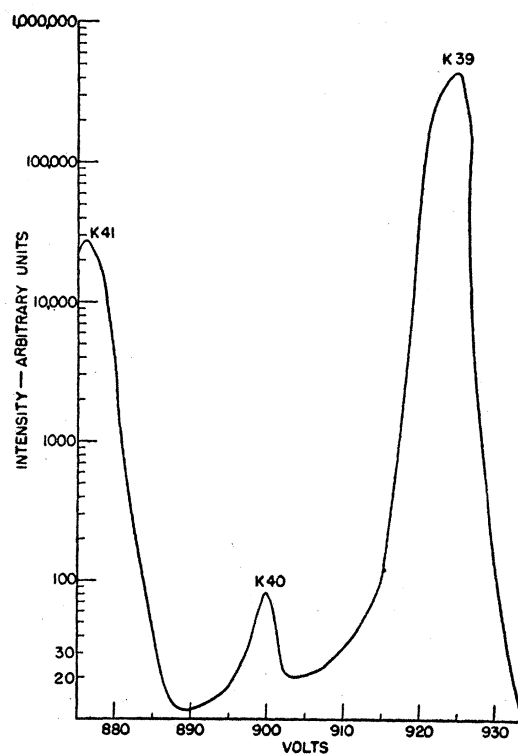


FIG. 5. The curve illustrates the resolution obtained in the mass spectrometer.

724A frequency meter was used to measure frequencies below 2 Mc/sec. Since the tunable frequency was always known to better than 1 kc/sec, this was also the accuracy of the mixed signal. Figure 7 shows a block diagram of the frequency source.

V. EXPERIMENTAL PROCEDURE AND RESULTS

a. The Ratio of the Moments

It was shown in a previous section that the transitions $(9/2, -7/2) \leftrightarrow (9/2, -5/2)$ and $(7/2, -7/2) \leftrightarrow (7/2, -5/2)$ in K^{40} differ in frequency by $2g_I(K^{40})\mu_0 H/h$. Similarly the frequencies of the transitions $(2, -1) \leftrightarrow (2, 0)$ and $(1, -1) \leftrightarrow (1, 0)$ in K^{39} differ by $2g_I(K^{39})\mu_0 H/h$. In order to measure these two doublet separations to sufficiently high precision, the transitions had to be observed at high fields (~ 9000 gauss) where it was difficult to prevent the C field from drifting during the course of the measurement of the four transitions. The following method of taking data was therefore adopted. The two K^{40} transitions were measured alternately and repeatedly; the time of each observation was recorded. Then the mass spectrometer was retuned, and the two K^{39} transitions were similarly measured. This procedure was repeated several times. The resonance frequencies of the four transitions were then plotted as functions of time and straight lines were drawn through the points belonging to the same transition. All points were less than one kc/sec from the best straight lines, showing that the C field drifted very nearly linearly during the course of a run. The resonance frequencies of all four transitions for particular times, and therefore

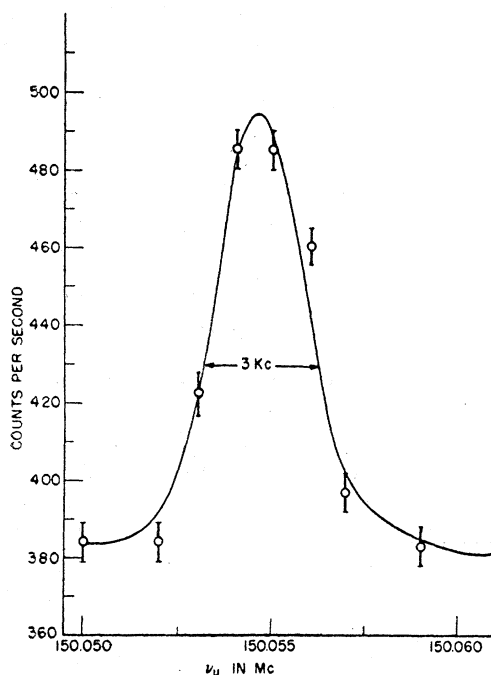


FIG. 6. Resonance curve of the transition $(9/2, -7/2 \leftrightarrow 9/2, -5/2)$ in K^{40} . The half-width of the curve is seen to be 3 kc/sec.

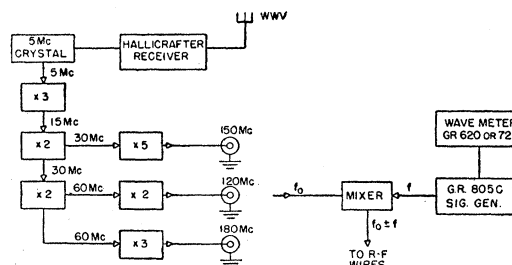


FIG. 7. Block diagram to illustrate the method employed to obtain radiofrequency currents with stable, variable frequencies in the ranges required for the present experiment.

belonging to the same field, were taken from these curves and are listed in Table I. The average value of $\delta\nu(K^{40})/\delta\nu(K^{39})$ obtained from these data is 1.24350 ± 0.00024 , where the quoted error is the average deviation from the average of all measurements.

Different A and B fields are required to render the K^{39} and K^{40} transitions observable. It was therefore necessary to determine the effect of stray A and B fields on the C field. This was done by studying a strongly field dependent line $[(2, -2) \leftrightarrow (2, -1)]$ in K^{39} as a function of A and B fields. It was found that the effect on the C field of a change in the deflecting fields, from the values required for K^{39} transition to those used for K^{40} transitions, is only 4 parts in 10^5 at 9000 gauss.

Applying this small correction factor, we obtain $g(K^{40})/g(K^{39}) = -1.24346 \pm 0.00024$.

b. The Measurement of $\mu_I(K^{40})$

The frequencies of the components of the K^{40} doublet corresponding to a particular magnetic field were measured by a method similar to the one mentioned before. From the mean frequency of the doublet, x was calculated by use of the Breit-Rabi formula [Eqs. (5) and (6)]. Knowing x , the doublet separation $\delta\nu(K^{40})$ yields $\mu_I(K^{40})$.

Values of μ_I at different values of H were obtained in this manner. At each field, the C field was allowed to drift for several hours, while the doublet frequencies were repeatedly measured. Figure 8 shows a portion of the data taken during one such run. The values for the moment obtained in the course of each run were averaged to give the values of μ_I quoted in Table II. The weight assigned to each run was determined by the magnitude of x as well as the number of individual measurements made during the run.

The weighted average value for $\mu_I(K^{40})$ is -1.2964 ± 0.0004 nm, where the quoted error is the average deviation of the 5 runs. From this, $g(K^{40}) = -0.32410 \pm 0.00010$. The diamagnetic correction to be applied to potassium is $+0.13$ percent.¹⁷ Including this correction, $\mu_I(K^{40})$ becomes -1.2982 nm.

¹⁷ W. E. Lamb, Phys. Rev. **60**, 817 (1941).

TABLE I. Data obtained during experiments for measuring $g(\text{K}^{40})/g(\text{K}^{39})$.

Run	Time	K^{40}			K^{39}			$\frac{\delta\nu(\text{K}^{40})}{\delta\nu(\text{K}^{39})}$
		ν_+ Mc/sec	ν_- Mc/sec	$\delta\nu$ Mc/sec	δ_+ Mc/sec	δ_- Mc/sec	$\delta\nu$ Mc/sec	
1	15	150.1530	145.9298	4.2232	117.6686	114.2702	3.3984	1.24270
	20	0.1562	0.9378	4.2184	0.6673	0.2723	3.3950	1.24253
	25	0.1614	0.9450	4.2164	0.6661	0.2745	3.3916	1.24319
	30	0.1654	0.9525	4.2129	0.6648	0.2767	3.3881	1.24344
	35	0.1692	0.9600	4.2092	0.6636	0.2790	3.3846	1.24363
	40	0.1730	0.9677	4.2053	0.6624	0.2811	3.3813	1.24369
	45	0.1763	0.9752	4.2011	0.6611	0.2833	3.3778	1.24374
	50	0.1792	0.9827	4.1965	0.6599	0.2855	3.3744	1.24363
	55	0.1816	0.9900	4.1916	0.6587	0.2877	3.3710	1.24342
2		150.0837	145.7583	4.3254	117.6961	114.2187	3.4774	1.24385
3	15	150.0523	145.6820	4.3703	117.7092	114.1950	3.5142	1.24361
	20	0.0546	0.6875	4.3671	0.7082	0.1967	3.5115	1.24366
	25	0.0567	0.6932	4.3635	0.7072	0.1985	3.5087	1.24362
	30	0.0591	0.6991	4.3600	0.7062	0.2002	3.5060	1.24358
	35	0.0614	0.7054	4.3560	0.7052	0.2021	3.5031	1.24347
	40	0.0639	0.7118	4.3521	0.7042	0.2041	3.5001	1.24342
	45	0.0666	0.7182	4.3484	0.7031	0.2062	3.4969	1.24350
	50	0.0692	0.7242	4.3450	0.7020	0.2083	3.4937	1.24367
	55	0.0719	0.7310	4.3409	0.7007	0.2106	3.4901	1.24377
	60	0.0746	0.7375	4.3371	0.6994	0.2129	3.4865	1.24397

Average: 1.24350 ± 0.00024

c. The Measurement of $\Delta\nu(\text{K}^{40})$

While the measurement of $g(\text{K}^{40})/g(\text{K}^{39})$ is limited essentially only by the accuracy of the frequency measurement, the value of $\mu_I(\text{K}^{40})$, which is obtained by use of the Breit-Rabi formula, depends on g_I and $\Delta\nu$. g_I is known to sufficient accuracy for our purposes (the value used in the present calculations is $2(1.001145)$), but the best determination of $\Delta\nu(\text{K}^{40})$ to date⁷ had an error of 0.050 Mc/sec assigned to it. The resultant uncertainty in μ_I is 0.001 nm, an error greater than the error introduced by the measurement of the two transition frequencies. A redetermination of $\Delta\nu(\text{K}^{40})$ was therefore desirable.

The frequencies of both components of the doublet ($F=I \pm \frac{1}{2}, -7/2 \leftrightarrow F=I \pm \frac{1}{2}, -5/2$) pass through a maximum at $x \approx 1.5$. By observing both these transitions in the neighborhood of this field, the maximum of the mean frequency $\bar{\nu}_{\max}$ can be measured. $\bar{\nu}_{\max}$ is about 193 Mc/sec. Since $\bar{\nu} = \frac{1}{2}\Delta\nu[(1+x^2)^{-\frac{1}{2}} - (1-x+x^2)^{-\frac{1}{2}}]$, the value of x corresponding $\bar{\nu}_{\max}$ is found by differentiation to be $x_0 = 1.466037$. $\Delta\nu$ can now be calculated from a knowledge of $\bar{\nu}_{\max}$. The percentage error of $\Delta\nu$ is equal to that of $\bar{\nu}_{\max}$, which was measured to an accuracy of about 1 part in 200,000. Table III shows the results of two runs of the type described above as well as the results of previous measurements. It is seen that the new value of $\Delta\nu(\text{K}^{40})$ overlaps the older results.

d. The Moment of K^{39}

By combining our results for $g(\text{K}^{40})/g(\text{K}^{39})$ and $\mu_I(\text{K}^{40})$, a value of $g(\text{K}^{39})$ can be calculated. We obtain $g(\text{K}^{39}) = 0.39097 \pm 0.00015$ nm. Collins⁹ has applied the nuclear induction technique to K^{39} , with a saturated aqueous solution of KNO_2 as a sample. His result is $g(\text{K}^{39})/g(\text{H}^1) = 0.13999 \pm 0.00002$. With Gardner and

Purcell's value for the proton moment,¹⁸ $g(\text{K}^{39}) = 0.391048 \pm 0.000070$ nm. Our value is in agreement with this result. Since Collins' measurement made no allowance for possible chemical effects on the position of the resonance, we conclude that the chemical corrections are smaller than the experimental uncertainties.

e. The HFS Anomaly

From Eq. (3) the hfs anomaly is given by

$$\Delta = \epsilon(\text{K}^{39}) - \epsilon(\text{K}^{40}) = \frac{\Delta\nu(\text{K}^{39}) g(\text{K}^{40})}{\Delta\nu(\text{K}^{40}) g(\text{K}^{39})} - 1.$$

With Kusch and Taub's⁸ value for $\Delta\nu(\text{K}^{39})$ of 461.723 ± 0.010 Mc/sec and the values for $\Delta\nu(\text{K}^{40})$ and $g(\text{K}^{40})/g(\text{K}^{39})$ obtained in the present experiment, we obtain $\Delta = (0.466 \pm 0.019)$ percent. This experimental value of Δ must now be compared with the Δ 's calculated on the basis of different nuclear models for K^{39} and K^{40} .

VI. COMPARISON WITH THEORY

a. The Bohr-Weisskopf Theory⁴

The hyperfine structure anomaly arises from the finite size of the nuclei and from the difference, in the

TABLE II. Results of six runs during which $\mu_I(\text{K}^{40})$ was measured at different magnetic fields.

Run	x	$\mu_I(\text{K}^{40})$	Weight
1	10.6	-1.2971	2
2	13.8	-1.2964	3
3	18.5	-1.2970	3
4	19.1	-1.2965	3
5	19.3	-1.2957	4
6	19.2	-1.2962	5

¹⁸ J. H. Gardner and E. M. Purcell, Phys. Rev. **76**, 1262 (1949).

two isotopes involved, between the distributions of the nucleon spins and currents which give rise to the nuclear moments. The magnetic hyperfine splitting, resulting from the interaction of the nuclear magnetic moment with the magnetic moment of an *S*-electron,† is given by the Fermi-Segrè formula, Eq. (1). For a nucleus of finite size, the factor $\mu_I |\psi(0)|^2$ must be averaged over the nuclear volume, and the resulting $\Delta\nu$ depends on the nuclear size, on the nuclear charge, and on the form of the distribution of the magnetic moment in the nucleus.

$$\Delta\nu_{\text{obs}}/\Delta\nu_{\text{pt}} = \langle \mu_I(r) |\psi(r)|^2 \rangle_{\text{Av}} / \mu_I |\psi(0)|^2 = 1 + \epsilon. \quad (9)$$

In particular, a nuclear moment caused by the intrinsic moments of one or more nucleons will cause a greater anomaly than a moment caused by orbital motion, since the moment arising from a current is strongly concentrated at the center of the nucleus. By a direct computation of the above average, assuming a spherically symmetrical distribution of moments and currents, Bohr and Weisskopf obtained

$$\epsilon = -(\alpha_s + 0.62\alpha_L) b(Z, R_0) \langle (R^2/R_0^2) \rangle_{\text{Av}}, \quad (10)$$

where α_s and α_L are, respectively, the fractions of the total nuclear magnetic moment as a result of spin and orbit

$$\alpha_s = (g_s/g) [(g - g_L)/(g_s - g_L)], \quad \alpha_L = 1 - \alpha_s. \quad (11)$$

$b(Z, R_0)$ is a parameter (taken as 0.19 percent for all the K isotopes) tabulated in the paper of Bohr and Weisskopf. Since the value of $|\psi(0)|^2$ cannot, in general, be computed with sufficient accuracy to determine ϵ from measurements on a given isotope, a comparison between experiment and theory can only be obtained from measurements of the ratios of the $\Delta\nu$'s and g_I 's for two isotopes of the same element (for which the $|\psi(0)|^2$ are assumed the same), as shown by Eq. (3).

The first set of measurements of the requisite accuracy resulted from the work of Bitter⁵ on the Rb isotopes, for which the measurement of the moment ratio, when compared with the previous measurement of the $\Delta\nu$ ratio by Millman and Kusch,¹⁹ showed an anomaly

$$\Delta(\text{Rb}) = \epsilon(\text{Rb}^{85}) - \epsilon(\text{Rb}^{87}) = (0.33 \pm 0.05) \text{ percent.}$$

Bohr and Weisskopf showed that the computed value of Δ is in satisfactory agreement with the measurements, provided that it is assumed that the nuclear moments result from the odd proton, with $g_s = 5.587$ and $g_L = 1$; the assumption of $g_L = Z/A$, on the other hand, gives a result in definite disagreement with the experiments.

† Since, for electrons with $L > 0$ (*p*, *d*, etc.), the electron wave function vanishes at the position of the nucleus, the finite nuclear size and/or distribution of spin and moment in the nucleus has negligible effect on the hyperfine structure. However, due to relativistic effects, the wave function of an electron in a $2p_{1/2}$ state has, for heavy nuclei, an appreciable $2s_{1/2}$ component and can, therefore, also give rise to an hfs anomaly.

¹⁹ S. Millman and P. Kusch, Phys. Rev. 58, 438 (1940).

TABLE III. Results of previous and the present measurements of $\Delta\nu(\text{K}^{40})$.

Zacharias* Davis <i>et al.</i> ^a		$\Delta\nu(\text{K}^{40})$, Mc/sec 1285.7 ± 0.1 1285.73 ± 0.05
Present work	Run No. 1	1285.786 ± 0.01
	Run No. 2	1285.794 ± 0.01
	Average	1285.790 ± 0.007

* See reference 7.

Another hyperfine structure anomaly measurement was made by Ochs, Logan, and Kusch,⁶ who compared the isotopes K³⁹ and K⁴¹ and obtained $\Delta_1(\text{K}) = \epsilon(\text{K}^{41}) - \epsilon(\text{K}^{39}) = (0.226 \pm 0.010)$ percent. Assuming, again, the g_s of a free proton, these authors observed that satisfactory agreement with the Bohr-Weisskopf (B-W) theory could only be obtained by assuming $g_L \approx 1$. The present experiments give $\Delta_2(\text{K}) = \epsilon(\text{K}^{39}) - \epsilon(\text{K}^{40})$.

Although the B-W theory makes no assumption as to the state of the odd proton (or neutron) responsible for the nuclear moment, the result—that $g_L \approx 1$ for the odd-proton nuclei investigated—lends support to an independent-particle model. However, the theory makes the assumption that the nucleon responsible for the moment is more or less uniformly (at least symmetrically) distributed throughout the nucleus, which would not be the case for a single-particle orbit. Furthermore,

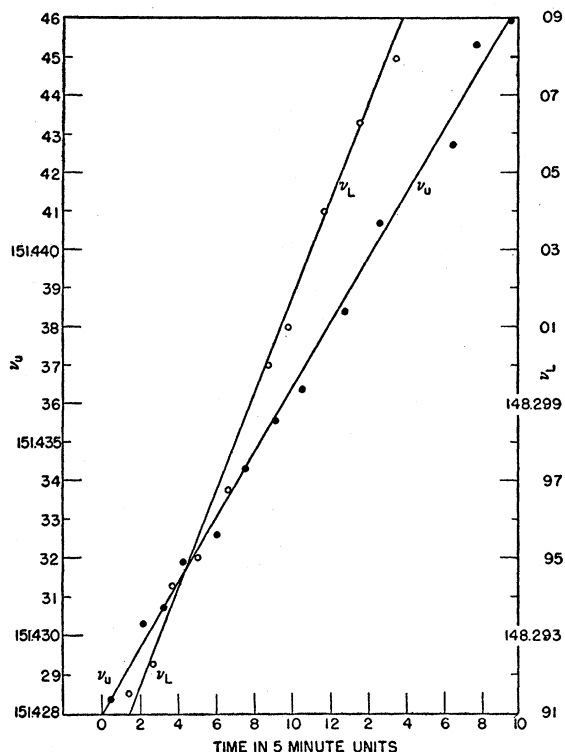


FIG. 8. The graph shows the resonance frequencies of the components of the K⁴⁰ doublet as a function of time while the C field was allowed to drift. The drift of the magnetic field is seen to be nearly linear over a period of two hours.

TABLE IV. Basic data on the spins and moments of the K and Rb isotopes.

Nucleus	I	Odd proton state	Odd neutron state	g (Schmidt)	g (measured)
K ⁴¹	$\frac{3}{2}$	$d_{\frac{3}{2}}$...	0.0826	0.14311
K ³⁹	$\frac{3}{2}$	$d_{\frac{3}{2}}$...	0.0826	0.2607
K ⁴⁰	4	$d_{\frac{3}{2}}$	$f_{7/2}$	-0.4209	-0.32412
Rb ⁸⁵	5/2	$f_{5/2}$...	0.3448	0.5406
Rb ⁸⁷	$\frac{3}{2}$	$p_{\frac{3}{2}}$...	2.5290	1.8314

the application of the B-W theory to odd-odd nuclei requires at least one further assumption concerning the mechanism of coupling between the neutron and proton spins and their orbital angular momenta in order to obtain the relative contributions to g . The necessary extensions of the theory, permitting its application to specific models, have been given by A. Bohr.

b. The Theory of A. Bohr^{20,21}

Bohr has shown that a more accurate theory of the hyperfine structure anomaly leads to the following modification

$$-\epsilon = [(1+0.38\zeta)\alpha_s + 0.62\alpha_L]b(Z, R_0)\langle(R^2/R_0^2)\rangle_{\text{av}}. \quad (12)$$

In this expression, α_s and α_L are as previously defined, $b(Z, R_0)$ is the same as in the B-W theory; $\langle(R^2/R_0^2)\rangle_{\text{av}}$ must be computed for the specific model under consideration, as must the constant ζ . In the case of the independent-particle model with spin-orbit coupling,²² Bohr obtained²¹

$$\begin{aligned} \zeta &= (2I-1)/4(I+1), & \text{for } I = L + \frac{1}{2} \\ &= (2I+3)/4I, & \text{for } I = L - \frac{1}{2}. \end{aligned} \quad (13)$$

For models such as those developed by Bohr,²⁰ in which the single particle is coupled to an asymmetric, rotating core, the expressions for ζ are more complicated.

In the following discussion, we compare the theoretical and experimental values of the hyperfine structure anomalies for a number of specific models; the comparison is shown for the K³⁹-K⁴¹ and Rb⁸⁵-Rb⁸⁷ anomalies as well as for the K³⁹-K⁴⁰ anomaly. The data on which the computations are based are given in Table IV. In addition, we use the values $g_p^{\text{free}} = 5.5870$, $g_n^{\text{free}} = -3.8270$.

Model 1a. We assume a strict single-particle model, with the odd nucleon in the state given in Table IV. The intrinsic moment of the odd nucleon is, however, assumed to be different from its free moment; its value is chosen to yield the observed nuclear moment with $g_L = 1$. Such a model has been proposed by Bloch,²³ by de Shalit,²⁴ and by Miyazawa.²⁵ The modifications of

the intrinsic moment could be a result of meson exchange currents in the nucleus.

K³⁹ and K⁴¹: for a $d_{\frac{3}{2}}$ proton, we take

$$g = \frac{\mathbf{S} \cdot \mathbf{I}}{I(I+1)}g_s + \frac{\mathbf{L} \cdot \mathbf{I}}{I(I+1)}g_L = -\frac{g_p^{\text{eff}}}{5} + \frac{6}{5}.$$

With g (measured) from Table IV, we obtain $g_p^{\text{eff}}(\text{K}^{39}) = 4.6965$ and $g_p^{\text{eff}}(\text{K}^{41}) = 5.2845$. Furthermore, for a $d_{\frac{3}{2}}$ proton, $\zeta = 1$ and $\langle(R^2/R_0^2)\rangle_{\text{av}} \cong 0.66$; $-\epsilon = (1.38\alpha_s + 0.62\alpha_L)(0.19)(0.66)$ percent, with $\alpha_s = -g_p^{\text{eff}}/5g$, $\alpha_L = 1 - \alpha_s$. The results are shown in column 3 of Table V.

K⁴⁰: Coupling a $d_{\frac{3}{2}}$ proton and an $f_{7/2}$ neutron to give $I = 4$ yields

$$g = \frac{\mathbf{I}_p \cdot \mathbf{I}}{I(I+1)}g_p + \frac{\mathbf{I}_n \cdot \mathbf{I}}{I(I+1)}g_n = \frac{g_p(d_{\frac{3}{2}})}{5} + \frac{4g_n(f_{7/2})}{5}.$$

Assuming $g_p(d_{\frac{3}{2}}) = g(\text{K}^{39}) = 0.2607$ and $g_L = 0$ for the neutron, we compute g_n^{eff} from $g_n(f_{7/2}) = g_n^{\text{eff}}/7$ and the experimental $g(\text{K}^{40})$; $g_n^{\text{eff}} = -3.2923$.

For the proton, the constants are as in K³⁹; for the neutron, $\zeta = \frac{1}{3}$ and $\langle(R^2/R_0^2)\rangle_{\text{av}} \cong 0.85$, whence $-\epsilon = (1.38\alpha_{sp} + 0.62\alpha_{Ln})(0.19)(0.66)$ percent + $(1.124\alpha_{sn}) \times (0.19)(0.85)$ percent with $\alpha_{sp} = -g_p^{\text{eff}}(\text{K}^{39})/25g$, $\alpha_{Ln} = 6/25g$, $\alpha_{sn} = 4g_n^{\text{eff}}/35g$. The result is shown in column 3 of Table V.

Rb⁸⁵: for an $f_{5/2}$ proton, $g = -g_p^{\text{eff}}/7 + 8/7$, $\zeta = \frac{4}{5}$, $\langle(R^2/R_0^2)\rangle_{\text{av}} \cong 0.80$; $b = 0.58$ percent for Rb. $-\epsilon = (1.304\alpha_s + 0.62\alpha_L)(0.58)(0.80)$ percent.

Rb⁸⁷: for the $p_{\frac{3}{2}}$ proton, $g = g_p^{\text{eff}}/3 + \frac{2}{3}$, $\zeta = \frac{1}{5}$, $\langle(R^2/R_0^2)\rangle_{\text{av}} \cong 0.49$; $b = 0.58$ percent, etc.

The results are given in column 3 of Table V.

Model 1b. The model is the same as 1a, except that we now ascribe the deviations from the Schmidt limits of the magnetic moments to a change in g_L , taking g_p^{free} and g_n^{free} as the intrinsic nucleon moments, and using the measured g to compute g_L^{eff} . (In this model, the neutron also has an effective orbital moment.) From the point of view of a meson theory, this model corresponds to the assumption that the meson currents affect only the orbital angular momenta. The results are shown in columns 5 and 6 of Table V.

Model 2. Feenberg and Davidson²⁶ have suggested another model which is less extreme in its "independent-particle" character. According to this model, the ground-state nuclear wave function is an admixture of a single-particle wave function (given s , L , and I) and a many-particle wave function, for which the total angular momentum I and the spin s are the same, but for which the orbital angular momentum differs from that of the single particle by one unit. Accordingly, the nuclear moment is made up of two parts (weighted according to the squares of the strengths of the re-

²⁰ A. Bohr, Phys. Rev. **81**, 134 (1951).

²¹ A. Bohr, Phys. Rev. **81**, 331 (1951).

²² M. G. Mayer, Phys. Rev. **78**, 16, 22 (1950).

²³ F. Bloch, Phys. Rev. **83**, 839 (1951).

²⁴ A. de Shalit, Helv. Phys. Acta **24**, 296 (1951).

²⁵ H. Miyazawa, Prog. Theoret. Phys. **6**, 263 (1951).

²⁶ Private communication. We thank Professor E. Feenberg for illuminating discussions on this problem.

TABLE V. Comparison between theory and experiment of the hfs anomalies of the K and Rb isotopes. All results are given in percent.

	Experiment Δ	Model 1a		Model 1b		Model 2		Model 3	
		ϵ	Δ	ϵ	Δ	ϵ	Δ	ϵ	Δ
K ⁴¹	0.226±0.010	0.626	0.360	0.666	0.335	0.632	0.357	0.396	0.231
K ³⁹	0.466±0.019	0.266	0.520	0.331	0.611	0.275	0.541	0.165	0.43
K ⁴⁰		-0.254		-0.280		-0.266		-0.26	
Rb ⁸⁵	0.33 ±0.05	0.066	0.325	0.181	0.489	0.085	0.343	0	0.26
Rb ⁸⁷		-0.259		-0.308		-0.258		-0.26	

spective contributions to the wave function). The first is the Schmidt limit corresponding to a single nucleon; the second is the opposite Margenau-Wigner²⁷ limit ($g_L = Z/A$) for the same I . The proportions of the two types of contribution are chosen to fit the observed nuclear moment. We illustrate by considering K³⁹ for which we take $g = ag_{\text{Sch}}(d_{\frac{3}{2}}) + (1-a)g_{\text{M-W}}(p_{\frac{3}{2}})$ with $g_{\text{Sch}}(d_{\frac{3}{2}}) = 0.0826$ and $g_{\text{M-W}}(p_{\frac{3}{2}}) = 2.1790$. Thus, for $g = 0.2607$, we obtain $a = 0.915$. The computation of the hfs anomaly now proceeds in a straightforward fashion

$$-\epsilon = (1.38\alpha_{s, \text{Sch}} + 0.62\alpha_{L, \text{Sch}})(0.19)(0.66) \text{ percent} \\ + (\alpha_{s, \text{M-W}} + 0.62\alpha_{L, \text{M-W}})(0.19)(0.60) \text{ percent,}$$

where $\alpha_{s, \text{Sch}} = -ag_p^{\text{free}}/5g$, etc. In the above, b is (as always) taken to be independent of the model; $\zeta = 0$ and $\langle(R^2/R_0^2)\rangle_n \cong 0.60$ for a uniform, spherically symmetrical spin distribution.

In applying the Feenberg model to K⁴⁰, we have assumed that $g = (1/5)g_p' + (4/5)g_n'$ with

$$g_p' = g(\text{K}^{39}) = a_p g_{\text{Sch}}(d_{\frac{3}{2}}) + (1-a_p)g_{\text{M-W}}(p_{\frac{3}{2}}); \\ g_n' = -0.47033 = a_n g_{\text{Sch}}(f_{7/2}) + (1-a_n)g_{\text{M-W}}(g_{7/2}).$$

The computation of (K⁴⁰) then proceeds as outlined above. The results of the application of the Feenberg model to the five nuclei under consideration are given in columns 7 and 8 of Table V.

Model 3. A. Bohr has developed a nuclear model in which the odd nucleon is assumed to be coupled to a symmetric, rotating nuclear core.²⁰ Depending on the nature of the coupling between the odd nucleon and the core, different values of the nuclear moments can be obtained. In general, the magnetic moments computed by Bohr are in fair agreement with the observed values.

The application of this model to the computation of the hyperfine structure anomaly has been discussed by Bohr²¹ for the K^{39,41} and Rb^{85,87} isotopes. The results are reproduced in columns 9 and 10 of Table II. Bohr²⁸ suggests the following asymmetric model for K⁴⁰: The nucleus is deformed into an oblate shape (negative quadrupole moment) under the influence of the $f_{7/2}$

neutron. The missing $d_{\frac{3}{2}}$ proton will then prefer to go into a state of $m = \frac{1}{2}$ with respect to the nuclear axis, leading to $I = 4$. The resulting g factor turns out to be -0.28 , in comparatively good agreement with the observed value (see Table IV). (This is a case of extreme coupling; partial decoupling of L and s for the odd nucleons might lead to even better agreement.) For this model, Bohr has computed $\epsilon(\text{K}^{40}) = -0.26$ percent, as given in column 9 of Table V.

c. Discussion

Comparison of the computed and measured hfs anomalies in Table V indicates: (1) qualitative agreement for all three models, (2) closest quantitative agreement with the model of Bohr (model 3), and (3) poorest agreement with model 1(b). This last is perhaps not too surprising, since this method of computation (ascribing the deviations of g from the Schmidt limits to an anomalous g_L) leads to values of g_L^{eff} that are critically dependent on the nuclear state; the same is not true of model 1a, for which the computed values of g_s^{eff} are fairly consistent.

Perhaps the most surprising result is the close agreement between the predictions of models 1a and 2, even for the case of Rb, where the deviations of the moments from the Schmidt limits are not inconsiderable. It is interesting to note, in this respect, that models 1a, 2, and 3 differ appreciably only in their predictions for K³⁹ and K⁴¹. Indeed, it is only on the basis of the hfs anomaly for these nuclei that it is possible to make any choice between the three models.

The major conclusion, however, is that the available data on the hfs anomalies gives strong support to nuclear models which are, in their essential features, based on the independent-particle model with spin-orbit coupling. The problem of the nature of the coupling between an odd proton and an odd neutron is, however, not particularly elucidated by the K⁴⁰ measurement, since the predicted ϵ for the models employing j - j coupling (1 and 2) and for the model of Bohr (3) are so closely alike. It is to be hoped that measurements on other odd-odd nuclei will shed more light on this question.

The authors gratefully acknowledge the guidance and aid of Professor J. R. Zacharias.

²⁷ H. Margenau and E. P. Wigner, Phys. Rev. **58**, 103 (1940).

²⁸ Private communication. We are indebted to Dr. A. Bohr for making these results available to us.